

This is a “preproof” accepted article for *Clay Minerals*.  
This version may be subject to change during the production process.  
10.1180/clm.2025.8

## **The clayey deposit from Bomkoul (Douala, Cameroon): a case study of geotechnical appraisal and assessment of firing brick’s characteristics**

Nzeukou N. Aubin<sup>1\*</sup>, Tchakouteu M. Theophile<sup>2</sup>, Mache J. Richard<sup>3</sup>, Lemougna N. Patrick<sup>2,4</sup>, Tsozué Désiré<sup>1</sup>, Meriam El Ouahabi<sup>5</sup>, Nathalie Fagel<sup>6</sup>, Chinje Uphie<sup>7</sup>

1: *University of Maroua, Faculty of Science, Department of Earth Sciences*

2: *University of Ngaoundéré, School of Chemical Engineering and Mineral Industry, Department of Mineral Engineering*

3: *University of Ngaoundéré, Department of Mining Engineering, School of Geology and Mining Engineering, Meiganga,*

4: *Faculty of Technology, Fiber and Particle Engineering Unit, University of Oulu, PO Box 4300, 90014, Finland*

5: *ESA, Saint-Luc, Liège*

6: *University, of Liege, Faculty of science, Department of Geology*

7: *University, of Yaoundé 1, Faculty of science, Department of Inorganic chemistry*

Submitted: 14 November 2024. Revised 15 March 2025. Associate Editor: Michele Dondi

\*Corresponding author: [nzeuk@yahoo.fr](mailto:nzeuk@yahoo.fr)

### **Abstract**

This study investigates two clayey facies from Bomkoul area in the littoral region of Cameroon for their suitability as fired clay building products. Field study consisted of geological survey and geotechnical mission (G0). Assessment of the raw clayey materials included mineralogy, particle size, determination of Atterberg limits, density and shear stress. Firing properties (shrinkage, water absorption and flexural strength) between 900 to 1100°C were also determined. The two main facies observed in the field are the mottled red/yellow grey clays from surface “A” with a thickness of 2-2.5 m and the deep blackish fossiliferous schisteous grey clays “B” with 8-10 m thick. Estimation based on boreholes revealed a minimum of 1.400.000 tons of clayey materials. These reserves will supply a small brick manufacturing unit for a minimum period of 25 years at an extraction rate of 50.000 tons per year. Main clay minerals are kaolinite (35 and 49%) and illite (1-11%). Both samples contain quartz (47 and 49%) as non-clay minerals, associated with a small amount of anatase (2.6-0.5%) and trace (<1%) hematite. The major oxides are SiO<sub>2</sub> (71-76%) and Al<sub>2</sub>O<sub>3</sub> (14%). The raw clayey material “A” was finer and more plastic than the “B” facies. The technological properties of the fired bricks obtained from the “A” facies were more interesting than the “B”

facies. A mixture made of 40% “A” and 60% “B” yielded satisfactory brick properties at 1050°C.

Keywords: clayey deposit, geotechnical mission (G0), firing properties, Douala, Cameroon.

## INTRODUCTION

Clayey materials are the basic raw material for brick making. For such ceramic applications, clayey materials should be neither too lean nor too greasy. They should dry easily with limited shrinkage and should be fired without problems. Pretreatment and use of admixtures can improve the efficiency and use of the clayey materials in various industrial processes (Konta and Kühner, 1997; Reeves et al., 2006; Christidis, 2011). The final mixture is often the result of careful and continuous research and the application of theoretical knowledge, but direct experience has often proven to be the most valuable. In the first phase of processing of raw material, it is sometimes necessary to reduce particle size by crushing and grinding. The resulting powder is then mixed and homogenized. The few key elements that should be considered when designing the production unit are: (i) mineral and chemical characteristics of the raw materials, (ii) natural state and workability of raw materials, (iii) the particle size distribution curve, etc (Manning, 1995; Dondi, 1998; Reeves et al., 2006). These characteristics vary according to the geological environment, which is controlled by the primary sources during *in situ* when alteration of primary rocks (residual clays) or by transportation and deposition (sedimentary or alluvial clays) (Wilson, 1998). The abundance of clay minerals (kaolinite, illite, smectite and chlorite) and non-clay minerals (quartz, feldspars, hematite, carbonates, etc.) present may differ among different clay types, and will affect the technological properties of the derived products. In Cameroon’s basement, various clays (sedimentary, residual and alluvial) are observed in different regions (Ngon Ngon et al., 2012a; Nzeukou et al., 2013). Residual clays, known as lateritic clays, are preferentially observed in the southern part of the country, consisting mainly by quartz, kaolinite and iron oxides (Thibault et Leberre, 1985; Ngon Ngon, 2012a). In this context, flux agents are necessary to improve the sintering behaviour of the fired products originating from these raw materials. Fired products obtained from lateritic clays of Yaounde presented dull sound, and flexural strength values between 2 and 8 MPa (Tibault et Leberre, 1985). These properties could be improved to reach 20 MPa at 1050°C by adding alluvial clays with lower melting point (Ngon Ngon et al., 2012a). In the northern regions of the country, clayey deposits contain smectite, carbonates and some flux oxides (alkali and alkali-earth) which impact the

technological behaviour of these clays. Tsozue et al. (2017) obtained good technological properties (bulk density  $1.8\text{g/cm}^3$ , linear shrinkage  $<5\%$ , flexural strength  $>5\text{MPa}$ , water absorption  $<13\%$ ) of fired products (at  $1000^\circ\text{C}$ ) from clayey materials of Maroua area. In the coastal or littoral region of the country, sedimentary clayey materials observed are essentially kaolinitic with minor quartz, illite and iron oxides, associated with minor carbonate and pyrite impurities (Ngon Ngon et al., 2012a; Kankao et al., 2022). The properties of derived ceramic products from these clays vary with the sintering temperature (Elimbi et al. 2014). At the Bomkoul area at Douala where red and grey clay facies are observed, the relatively high amount of alkaline oxides favour clay maturation at lower temperatures (Elimbi and Njoupouo, 2002; Elimbi et al., 2014). The mottled red clay facies is mainly used to produce floor and wall tiles, and despite admixture with low-grade clay, the resulting ceramics quality are satisfactory (Elimbi et al., 2014).

The first studies on assessment of clayey materials for fired products in the Littoral region of Cameroon were performed by the French “Bureau de Recherche Géologique et Minière” (BRGM), in 1980 as part of the project “Study and mining prospection of South-West Cameroon” (Thibaut & Le Berre, 1985). The most important clay deposits in terms of quality and reserves were discovered in Mbanga, Kilometric point 7.5 and 17 (PK7.5 and PK17) and, Koungue and Dizangue between Douala and Edea (Fig. 1). Except for the PK17 deposit at Bomkoul, the thickness of the sand cover (5 to  $>30$  m) was the limiting factor for detailed studies. In the framework to set up an earth brick industry in Douala in 1982, the PK17 clayey deposit has been quantitatively estimated to have  $\sim 1000000\text{ m}^3$  of clayey material, with a possibility to supply a unit using  $30.000\text{ m}^3$  of clayey material per year for a period of 30 years (Thibaut & Le Berre, 1985). Some studies examined the use of these clayey materials as raw materials for ceramics (Thibaut & Le Berre, 1985; Ngon Ngon et al., 2012b; Elimbi et al., 2014). According to Thibaut and Le Berre (1985), Bomkoul’ clayey material has good extrusion properties and high green flexural strength. They could be exploited for the manufacture of clay bricks after firing at  $900\text{-}1000^\circ\text{C}$ , or ceramic tiles after firing at  $1200^\circ\text{C}$ . The first geological studies on the Bomkoul clayey material (Ngon Ngon et al., 2012b) showed the presence of heterogeneous clayey materials on hills (80-120 m altitude) with variable colours: grey, dark-grey and mottled. The clayey deposits are thick at the upper slope and thin at the middle and lower slopes. Their textures vary from sandy-clay, clayey-silt and silty-clay to clay and they have a good potential for pottery and manufacture bricks, ceramic roofing tiles, wall and floor stoneware tiles (Ngon Ngon et al., 2012b). Previously, Elimbi and Njopwouo (2002) had suggested that the two facies of Bomkoul' clays have good firing

characteristics. Also, [Elimbi et al. \(2014\)](#) showed that adding at least 15% alkaline feldspar as a flux to mottled red clay facies give good properties for “*terra cotta*” when fired at temperature between 1050 and 1100°C. Addition of 25% of fluxes and firing temperature ~ 1200°C, yielded ceramic products with low water absorption (0.70% - 0.25%). Addition of the grey clay facies (10 to 50%) or alkaline feldspars to the red clay facies, had sufficient fluxing effect on compact ceramics at lower firing temperature ([Elimbi et al., 2014](#)). A ceramics factory was established in 1975 in the northern suburbs of Douala in Bonendalé, by the Industrial Ceramics Company of Cameroon (former CERICAM) and part of its clayey raw material came from the PK17 site in Bomkoul. However, the CERICAM Quarry (at Bomkoul site) currently occupied by residential houses and other infrastructures, which makes difficult and costly industrial exploitation. A geological survey at this reference site helped to identify and map the areas that can be exploited for the industrial production of clay bricks. Instead of the physicochemical and mineralogical traits presented in [Ngon Ngon et al. \(2012b\)](#), this work examines the geological and geotechnical features obtained from these raw materials found around the old CERICAM quarry. It also presents the reserve estimation of clayey materials available, the different formulations and the ideal firing temperature to obtain fired bricks with good properties.

## MATERIALS AND METHODS

### *Materials*

#### *Geological and geotechnical survey*

The study area is located at Bomkoul at PK 17 in the Douala 3<sup>rd</sup> subdivision (Cameroon, Central Africa) (Fig. 1, 2). Geologically, it belongs to the Douala sub-basin which is part of the large coastal sedimentary basin of Douala- Kribi-Campo ([Regnault, 1986](#); [Nguene et al., 1992](#); [SNH/UD, 2005](#); [Ngon Ngon et al., 2012b](#); [Sobdjou et al., 2023](#)). Seven major formations constitute the lithostratigraphy of the Douala sub-basin (Fig. 3a). The Bomkoul’s sedimentary materials belong to the Matanda-Wouri formation of Upper Tertiary Miocene-Pliocene age ([SNH/UD, 2005](#); [Ngon Ngon et al., 2012b](#)). The Matanda Formation is dominated by deltaic facies interstratified with volcanoclastic layers. The Wouri Formation consists of gravels and sandy deposits with kaolinic clayey materials ([Regnault, 1986](#); [SNH/UD, 2005](#); [Ngon Ngon et al., 2012b](#); [Sobdjou et al., 2023](#)).

A geological survey using a hand auger (S1 to S10) at about 4 km from the former Bomkoul clay extraction site by CERICAM (former CERICAM quarry) helped to identify a suitable clayey site for a detailed estimation of the reserve (Fig. 2, Table 1S). Three pits (P1 - P3)

about 10 m deep were dug and the description of the outcrops profile was made. To better estimate the vertical coverage of the in-situ materials, two mechanical boreholes (SPT1 and SPT2) up to 30 m deep, were drilled as part of a geotechnical survey (G0), conducted by the National Civil Engineering Laboratory (Labogenie), in accordance with the classification of geotechnical tasks (Eurocodes 7 Part 2 (EN 1997-2)) on the "Recognition of land and trials". This survey helped to define the different formations, their nature, the in-situ soil characteristics and the different groundwater levels. The reconnaissance drilling auger ROTARY 100 mm used is a SEDIDRILL 400 until 30 m deep in order to perform SPTs at 1.50 m intervals (ASTM D 1586-99). The boreholes also helped to collect undisturbed samples of loose soil for identification with SHELBY tubes. Boreholes S7 and S8 are towards the eastern limit of the deposit (Fig. 2). S1 is located in the ancient CERICAM quarry while S2, S3 and S4 are towards the northwestern limit on a different outcrop (NW neighbouring hill) of the main site. P3 and S5 lie on the crest, at the centre of the main site. P1 and the boreholes S9 and S10 are located on the sides of the main site and allowed to better estimate the thickness of the exploitable clayey layer. P2 was dug at the northeast of the deposit after the pathway.

Comment [U1]: Spell out

The surveys carried out show the following succession of formations from top to bottom (Table IS):

1. a lateritic breastplate layer, compact and clayey at the base, 0-1.5 m thick;
2. a mottled red/yellow-grey clay, layered and laminated, fine in texture with nodules, and thickness varying from 0.9 to 4 m;
3. a blackish grey clay with laminated structure, fine and very compact, plastic and fairly homogeneous, with fossils, and thickness varying from 3.5 to 14.5 m;
4. and a sandy layer with various characteristics, from 12.5 to 30 m.

Two major facies characterize the Bomkoul clayey deposit: the mottled red/yellow grey and the blackish grey facies, in accordance with the Ngon Ngon et al. (2012b) and Elimbi et al. (2014). However, Ngon Ngon et al. (2012b) in their study considered three clayey facies: mottled, grey and dark grey. The dark grey and grey clays likely correspond to the blackish grey ones observed in this study while the mottled clay corresponds to the mottled red/yellow grey facies. Following the description terminology of Miall (1990) and Walker (2006), the main sedimentary structures observed on the clayey layers are laminations. The collected sample tubes were sealed with wax and protected before being sent to the laboratory. Approximately 2 to 3 kg of samples were collected for analysis that included: granulometric

test (NF P 94-041), moisture content (NF P 050), Atterberg limits (NF P 94 051), apparent density (NF P 94 053), specific density (NF P 94 054) and shear stress test (NF P 94 071-1).

*Bomkoul's clayey deposit: site topography, description and reserve estimation*

The city of Douala is located in the sedimentary basin made up of Neogene ((Miocene-Pliocene) and Lower Quaternary deposits. Due to the very humid and hot climate, weathering is deep, and morphological differentiations are quite similar from one sector to another. The Cretaceous outcrops have yielded either friable, fine to coarse sandstones with intercalations of kaolinitic sandstones, calcareous or marly, which after weathering present sandy, sandy-clayey or clayish-sandy yellow or mottled surface textures (Ngon Ngon et al., 2012b; Kankao et al., 2022; Sobdjou et al., 2023). The Bomkoul's clayey deposit is bare and for the most part devoid of original vegetation. The site had been quarried for its laterite cover, thus leaving the underlying clayey layer nearly exposed. The altitude of the deposit varies between +26.00 and +20.00 m NGF GPS. The clayey site is a half dome with its slope westward, consisting of a NS oriented main block (348 m long and 130- 220 m wide with an extension to another block at the NW. Both blocks constitute an elongated low dome, with relative altitude ranging in relative altitude from about 6 m to 32 m (GPS Data, Fig.1c) above sea level.

The area of the deposit is approximately 6 ha. Following the morphology of the site, the spacing between pits and boreholes is ~ 200 m. Figure 2 shows the sampling points and drilling position, and Figure 3 presents the schematic cross-section of different profiles and their description. In general, field observations align with the literature data and the findings of the general geological study. The clayey materials observed in the field are shales altered on the first meter's depth and seem to belong to the series of the Tertiary shale series of the Douala's basin (Ngon Ngon et al., 2012b; Sobdjou et al., 2023). The clayey layers are generally covered by nodular breastplates more or less argillaceous ~1m thick, which are lateritic layers assessed for roadworks.

The subsoil of the Bomkoul clayey site therefore has a geological structure that can be described as globally homogeneous, with local inhomogeneity both on the surface and in depth. The profiles correlate very well. The average thickness of the mottled reddish/yellow grey and black-greyish plastic clays of boreholes SPT 1 and 2, is ~ 3.25 m and 10 m respectively. No other pits were deep enough to reach the bottom of the lower blackish (greyish) layer. However, the fairly good correlation of SPT 1 and 2 pits and boreholes allow a confident extrapolation from the complete profiles of the later. With the SPT 1 and 2

mechanical drilling data, the thickness of the exploitable layer varied from 2 to 2.5 m for facies “A” and 8.5 to 11.5 m for facies “B” (Fig. 3b). Following field observations and considering a minimum exploitable clayey material thickness, of 2 m for facies A and 8.5 m for facies B, for the average 6 ha of the Bomkoul clayey site a minimum the following reserves were estimated: 120.000 m<sup>3</sup> from facies A and 510.000 m<sup>3</sup> from facies B (Table 1). Considering an average of 1.60 tons/m<sup>3</sup> of materials, the reserves are: 192.000 tons of clayey materials from facies A and 816.000 tons from facies B. Considering a consumption rate of 50.000 t/y, this deposit could operate for more than 4 for facies A and 16 years for facies B (Table 1).

#### *Raw materials and brick making preparation*

Preparation of fired bricks with Bomkoul’s clayey materials was carried out using the two major facies observed: the mottled reddish/yellow grey facies (about 5m denoted as sample “A” and, the blackish grey depth facies (more than 10 m thick) denoted as sample “B” (Fig. 1S).

#### *Mineralogical and chemical analyses*

X-ray diffraction (XRD) analysis was carried out with a Bruker Advance D8 ECO diffractometer (Cu K $\alpha$ 1 radiation,  $\lambda= 1,5418 \text{ \AA}$ , 40 kV, 30 mA) at the AGEs laboratory (ULiège, Belgium). Sample preparation followed the methodology of Moore and Reynolds (1989). After grinding (< 80 $\mu\text{m}$ ), a small sample was placed on sample holder by front loading to reduce preferential orientation. The < 2 $\mu\text{m}$  fraction was separated by settling in a water column; the samples were mounted as oriented aggregates on glass slides and three X-ray patterns were recorded on each sample: air dried, glycolated (24 hours) and heated (500°C for 4 hours). The measurements were carried out in the 2 $\theta$  range from 2° to 70°, with a step size of 0.02° and a time per step of 2 s. Mineral phase identification and quantification were performed using Bruker®Eva and Topas software. The Rietveld refinement method, implemented on Topas (Bruker) software (Fig. 2S) was applied to all the minerals phases identified by XRD. The methodology, including reference standard and instrumental limitations, is according to Fagel et al. (2024a, 2024b). Fourier transform infrared (FTIR) spectroscopy was used to complement the XRD results. The FTIR Spectra were recorded in the range 4000 and 400 cm<sup>-1</sup> on a Bruker® alpha-P spectrometer using KBr pellets. The infrared spectroscopy was fulfilled with a resolution of 4 cm<sup>-1</sup> between 4000 and 400 cm<sup>-1</sup>

wavenumbers with a Bruker Nicolet Nexus at the Analytical Chemistry Laboratory in the University of Yaoundé I in Cameroon. The powdered sample was diluted in 180 mg of KBr and pressed to form pellets. The spectrum of pellet was recorded by accumulating 200 scans at a  $1\text{ cm}^{-1}$ . Simultaneous thermal analysis (STA) was performed on a TG-DSC instrument (SETARAM) with a heating rate of  $5^{\circ}\text{C}/\text{min}$  from ambient temperature to  $1200^{\circ}\text{C}$  at the AGEs laboratory, University of Liege, Belgium.

Chemical analyses were performed with X-ray fluorescence spectroscopy (XRF) with a Bruker S4 PIONIER XRF spectrometer on the  $< 250\ \mu\text{m}$  fraction of the samples. Powder pellets with a diameter of 34 mm and a thickness of 2.5 mm were compacted at 200 kN cold strength.

#### *Bricks preparation*

Two mixtures (M1, M2) were prepared for firing tests. M1 is a mixture of 40% facies “A” and 60% facies “B” while mixture M2, contains 60% of A facies and 40% of B facies. Before mixing, samples were dried, ground in a mortar to pass through a 1 mm sieve. 12% water was added to obtain paste with good consistency. After homogenization, specimens with dimensions  $8\times 4\times 2\text{ mm}$  were prepared with a hydraulic press (10 tons). Thereafter, specimens were dried at room temperature for few days, and in an oven ( $105^{\circ}\text{C}$ ) for 24 hours. Subsequently samples were fired at  $900^{\circ}\text{C}$ ,  $950^{\circ}\text{C}$ ,  $1000^{\circ}\text{C}$ ,  $1050^{\circ}\text{C}$  and  $1100^{\circ}\text{C}$ , with a heating rate of  $5^{\circ}\text{C}/\text{min}$  and a dwell time of 2 hours at maximum temperature. The colour, sound, linear shrinkage, bending strength and water absorption) were determined according to the NC 25-2010 standard.

## RESULTS AND DISCUSSION

### *Bomkoul's clayey deposit, major characteristics for fired brick evaluation*

#### *Mineralogy and chemistry*

Figure 4a shows the bulk XRD traces of samples A and B and Table 2 lists their chemical composition. The main minerals present are quartz (47 and 49%) and kaolinite (35 and 49%) for A and B samples, respectively, followed by illite (11 and 1%), muscovite (1.3 and 0.6%) and anatase (3 and 0.5%). K-feldspar (~2% microcline, 1.3% orthoclase and 0.4% sanidine) was detected only in facies A. In the less than  $2\ \mu\text{m}$  fraction (Figure 4b and c), no swelling minerals are observed in both samples. Illite and kaolinite are confirmed as the main clay minerals with main peaks at  $9.87\ \text{\AA}$  and  $7.15\ \text{\AA}$ , respectively. The chemical composition matches the quantitative mineralogical data. The 48% of quartz content and 35-49% kaolinite

**Comment [U2]:** Authors, this is unclear. What type of FTIR spectrometer did you use? You have to delete one of the two shown.

content explain the  $\text{SiO}_2$  and  $\text{Al}_2\text{O}_3$  contents (Table 2). The small amounts of  $\text{Fe}_2\text{O}_3$ , alkali and alkali-earth oxides observed in both facies (Table 2) are in line with the mineralogical composition. These results contradict Ngon Ngon et al. (2012b), who identified also smectite (17%), goethite (8%), calcite (7%), ilmenite (5%), pyrite (4%), gibbsite (4%), chlorite (4%) and hematite (3%). This difference is ascribed to site heterogeneity and difference in sampling locations, as the present study was conducted out of the ancient CERICAM area (Fig.1c), the study area of Ngon Ngon et al. (2012b). Bomkoul's clayey materials are more kaolinitic and reflect the kaolinitic clayey materials from Wouri formations mentioned by Regnault (1986). The environmental conditions of the Douala sub-basin show multiple sedimentary formations, which may influence the mineralogical content of clayey materials depending on the location. The FTIR spectra (Figure 5) are in accord with the XRD results. Samples A and B exhibited the stretching vibrations of structural-OH groups of kaolinite at 3691 and 3620  $\text{cm}^{-1}$ , and the bending modes at 907  $\text{cm}^{-1}$  (Saikia and Parthasarathy, 2010). The band at 1633  $\text{cm}^{-1}$  in sample A, being absent in sample B, corresponds to deformation of H-O-H bonds of water molecules. The bands at 1114, 1027 and 1001  $\text{cm}^{-1}$ , correspond to Si-O-Si and asymmetric Si-O-Al vibrations (Kakali et al., 2001; Tchakouté et al., 2013). The band between 3500 and 3000  $\text{cm}^{-1}$  in sample A, and the bands at 791, 748 and 678  $\text{cm}^{-1}$  may be attributed to the deformation of O-H, associated with illite.

Figure 6 shows the thermal behavior of samples A and B. Zone 1 shows a small endothermic peak at  $\sim 40^\circ\text{C}$  for material A and at  $65^\circ\text{C}$  for material B corresponding to the release of residual water from shaping (Baran et al., 2001). According to the TG curves, the mass losses associated with this transformation are not significant being approximately 1.5 and 0.5 wt% for A and B respectively. A small exothermic peak is observed at  $\sim 240^\circ\text{C}$  for profile A (zone 2), characteristic of the degradation of organic matter (Pialy et al., 2008).

The second endothermic event (zone 3), which is identical for the two clays studied, is observed between 480 and  $540^\circ\text{C}$  with very marked intensity. At this temperature range ( $400\text{--}600^\circ\text{C}$ ), kaolinite and illite undergo significant structural changes. Kaolinite transforms to nearly amorphous metakaolinite. This endothermic transformation is associated with a significant weight loss, approximately 4.5 wt% for A and 4.70 wt% for B. The significant weight loss observed is due to the dihydroxylation of clay minerals. The weak endothermic peak at  $\sim 573^\circ\text{C}$ , corresponds to the transformation of  $\alpha$ -quartz to  $\beta$ -quartz (Glover, 1995). The exothermic peak of zone 4 at  $\sim 977^\circ\text{C}$ , observed for the two clay raw materials, is due to the structural reorganization of the clay minerals (progressive transformation of metakaolin into mullite).

### *Physical properties of the clays*

The two major facies observed on the clayey deposit are: (i) the mottled red/yellow grey facies of surface (sample A) and (ii) blackish depth grey facies (sample B) intercalated sometimes by one thinner transition facies rich in shells and nodules. The mottled red/yellow clay facies are layered and laminated silty to sandy-clays, with finer texture (~80% of fines) and few gravels (~1.5%). The plasticity index of 20.4% and liquidity index between zero and one are likely to correspond to plastic materials. These facies correspond to the weathered materials with reddish-brownish spots/ferruginous nodules observed at the upper slope topography described by [Ngon Ngon et al. \(2012b\)](#). The blackish grey facies overlain by weathered clays present laminated structure, with sandy-clay texture (~87% of sand), plasticity index of 30%, and liquidity index value ~0.31 indicative of plastic state at the sampling time. These facies correspond to the compact laminated grey or dark-grey clays with muscovite and scattered moulds of gastropods of [Ngon Ngon et al. \(2012b\)](#). Table 3 lists the major technological characteristics of the two facies. Particle size distribution and consistency play a major role to understand the engineering properties of soils, ([Dondi et al., 1998](#); [Carretero et al., 2002](#); [Christidis, 2011](#)). The consistency is significantly influenced by the amount of water present in soil according to Atterberg limits. The undisturbed soil PEI-1 considered as "sample A", taken between 3.5 and 3.8 m from the SPT2 drilling point, has a natural water content ( $\omega$ ) of 41.4 wt% whereas the water content should be, in the case of normal humid soils, equal to the plastic limit ( $W_p$ ), i.e., 26.5 wt%. The moisture and dry unit weight values were ~ 16 and 11 kN/m<sup>3</sup> respectively. The material was very hydrated at the sampling time (weight of water around 5 kN). According to AASHTO classification, this soil is A-7-6 class. These are sensitive soils with high plasticity that can be very compressible with considerable volume change. The grading curve (Fig. 7a) covers a wide range of particle sizes ranging from gravel to fines. The fine fraction (silt + clay) is ~ 80.5% with the clay fraction (< 2 $\mu$ m) exceeding 75%. The sand and gravel fractions are 18 and 1.5 wt% respectively. Fine particles ( $\emptyset < 80\mu$ m) were ~80%, suggesting a heavy sandy clay which might cause problems like unsuitable agglomeration during processing ([Carretero et al., 2002](#)) or cracks appearing and excess shrinkage in firing products ([Reeves et al., 2006](#)).

The undisturbed soil (PEI-2), denoted as "sample B", that was collected 6.5-7.0 m away from the SPT1 drilling point, has natural water content ( $\omega$ ) 19.4 wt% whereas it have, in the case of normal humid soils, the water content of the plastic limit ( $W_p$ ), i.e., 10 wt%. The moisture

**Comment [U3]:** kN/m<sup>3</sup> is not a weight unit. N is a force unit

and dry unit weight values were  $\sim 19$  and  $16 \text{ kN/m}^3$  respectively. The material was very hydrated (weight of water around  $4 \text{ kN}$ ) at the sampling time. According to the AASHTO classification, this soil is A-2-4 class. These are sandy soils sensitive to small variations in water content, which may lose their cohesion in the event of an uncontrolled increase in water content. Fig. 7a shows that the particle size distribution curve of sample B did not include all the particle size fractions. The total of fines ( $< 80\mu\text{m}$ ) is 13.5%, probably including only the silt fraction. 86.5 % of sample B consists of sand fraction, which can be considered as a coarse-grained soil or as sandy material. It is a poorly/uniformly graded sample, with high plasticity value of 30%. The high plasticity may be attributed to the presence of illite in this material (Fig. 7b), in accordance with the  $\text{SiO}_2/\text{Al}_2\text{O}_3$  ratio which exceeds 2, suggesting the presence of a 2:1 phyllosilicate of illite type (Tsozué et al., 2017). Low plastic (PI  $< 10\%$ ) or highly plastic (PI up to 35%) materials, are not suitable for extrusion (Carretero et al., 2002; Jeridi et al., 2008; Wang et al., 2023). Also, the more one fraction is dominating, the more the grading curve will need to be well graded (Dondi et al. 1998). Sample A with  $W_p \sim 27\%$  and  $PI \sim 21\%$  may be suitable for extrusion, while sample B with  $W_p \sim 10\%$  and  $PI \sim 30\%$  may be acceptable (Fig. 7c). Sample A included particle size from gravel to clay, but the proportion of silt and sand need to be adjusted. Also, in sample B, the proportion of silt and clay need to be adjusted.

Sample A is a plastic material with plastic limit  $\sim 20 \text{ wt}\%$  and liquidity index of 0.7. This material needs at least 47 wt% water before flowing to its own weight. At this liquid stage, there is no shear strength in that material meaning no resistance. When the water content changed from the liquid to plastic state, the values of shear strength were 13 kPa and 17 kPa for sample A and sample B respectively (Fig. 8). The dynamic penetrometer test gives a continuous relative soil strength with depth (Abdulrahman, 2015). This variation of the resistance curve with depth also confirms the heterogeneity of the site materials. Facies A is less resistant and less cohesive material than facies B (Fig. 8). Plasticity index also confirms the lower cohesion of sample A (PI:20) compared to facies B (PI:30). Overall, the materials studied are of very dense consistency from 3.50 meters depth relative to the natural ground.

#### *Assessment of fired bricks*

The  $\text{Fe}_2\text{O}_3$  and  $\text{TiO}_2$  contents,  $\sim 1\text{-}3 \text{ wt}\%$  and  $1.5 \text{ wt}\%$  respectively, are responsible for the pink colour of the ceramic specimens after firing (Fig. 3S).

The sound of fired specimens obtained with the depth blackish grey facies B remained dull from  $900^\circ\text{C}$  to  $1100^\circ\text{C}$  while those obtained with 100% of the surface mottled facies A as

Comment [U4]:  $\text{kN/m}^3$  is not a weight unit. N is a force unit

Comment [U5]: See previous comment

Comment [U6]: Authors : This is unclear. Please clarify

Comment [U7]: Authors : Unclear. Clarify

well as mixtures M1 and M2, had a metallic sound at all firing temperatures. The cohesion is very good for all the specimens (Fig. 4S). The metallic sound in general reflects maturity of the fired products, showing that chemical transformation occurs during the sintering stage (Nzeukou et al., 2013; Dondi et al., 2001, Wang et al., 2023). The sound is produced when cohesion is high due to partial glass formation during sintering reactions and it assists in estimating the sintering maturity of a product (El Boudour El Idrissi, 2018; El Ouahabi et al., 2019). Facies A can be considered as able to achieve sintering maturity at lower temperature than facies B.

On drying (at 105°C), clayey materials of facies A shrink four to five times more than their counterparts of facies B (Table 4, Fig. 9). The Brick Industry Association (BIA) recommends drying shrinkage values 2-8% (El Idrissi et al. 2022). The values obtained from the studied samples were ~ 4-6% for surface mottled clayey material and 1-2% for depth blackish grey clayey material. The specimens from M1 and M2 mixtures have almost equal drying shrinkage values, and after firing, the shrinkage values are <2% at temperatures lower than 1050°C and 4% at 1100°C. The recommended values for firing shrinkage from BIA are 2-10% (El Idrissi et al., 2022). Facies A is rich in fine-grained material (80%), it is therefore more plastic than facies B. This property is beneficial for hand moulding shaping or extrusion process (Jeridi et al., 2008; Christidis, 2011; Wang et al., 2023). After firing, the “A” surface clayey material exhibited a higher shrinkage (3-5%) while the B depth clayey material exhibited very low shrinkage (<1%), with negative values at 900°C, 950°C and 1050°C. No cracks are observed on fired bricks specimens (Fig. 4S). Inasmuch as the linear shrinkage indicates firing efficiency, the low values obtained from facies “B” suggest a poor performance and strength for production of fired bricks. This is probably due to the lack of liquid-phase formation that would enhance densification reactions during sintering (Elimbi et al., 2014; Anianpour & Anianpour, 2022). The kaolinite content of this sample may be responsible for its refractory character. Suitable amount of flux mineral (K-feldspar) may favour its fusibility. Shrinkage values of facies “A” and mixtures M1 and M2 are lower than 8%. According to Wang et al. (2023), bricks with firing shrinkage less than 8% may be considered of good quality. Besides, Boussen et al. (2016) proposed firing shrinkage values less than 3% for good quality fired bricks.

The flexural strength of the fired specimens as a function of firing temperature is shown in Fig. 9. As the firing temperature increased, the flexural strength of the pieces also increased due to densification. The flexural strength varied between 0.6 MPa and 7.2 MPa achieving their maximum values at 1100°C. The clayey material B showed the lowest values (< 1MPa)

while the surface mottled clayey material A showed the highest values (6 to 7 MPa). The flexural strength values of M1 and M2 mixtures were 2.5-3.5 MPa with the M2 values being slightly higher than those of M1 at 950-1100 °C. This performance is probably due to the transformation reactions taking place from 950°C, with the proportion of mottled surface clayey material, reacting at lower temperature, being higher in M2 (60%) than in M1 (40%). The presence of illite, with fluxing oxides like K<sub>2</sub>O, Na<sub>2</sub>O, and possibly Fe<sub>2</sub>O<sub>3</sub> (Table 2) of the raw clay promoted sintering, which increased melt formation and densification of the fired products (Elimbi et al.,2014; Anianpour & Anianpour, 2022; Lemougna et al., 2024). Iron generally affects sintering kinetics and may enhance vitrification (Andji et al., 2009). The water absorption of fired specimens obtained with the mottled surface clayey material “A” showed a decreasing trend with the firing temperature, for both the M1 and M2 mixtures (Fig. 9). The evolution of water absorption is related to densification of fired products because porosity controls water absorption and affects strength of the fired bricks (Anianpour & Anianpour, 2022). Sintering of the ceramic specimens was accelerated above 900 °C as the glassy phase formed. The glassy phase penetrated the open pores, closing and isolating them from neighbouring pores. This explains the significant decrease of the water absorption after sintering at higher temperatures. However, from 1000 to 1050 °C, the water absorption values of specimens from the A facies increased from 16 to 18% before decreasing between 1050 and 1100 °C. For deep blackish grey clay B, the water absorption value increased to 21% at 1000 °C before decreasing thereafter. In the temperature range from 1000 to 1050 °C, there is a structural reorganisation which may enhance the porosity in firing products. Good quality ceramic products may be obtained at 1050°C (El Idrissi et al., 2022). Lower water absorption values (20-22%) were obtained with mixtures of M1 and M2 at 1000 °C. Water absorption is an important parameter to consider for fired bricks, but the appropriate values also depend on the target application and the weathering conditions. The ASTM C62-99 recommends water absorption below 17% for bricks exposed to severe weathering. Cameroonian’s norms NC23-2010 recommends a water absorption value < 20% for ordinary masonry and < 15% for foundation masonry. The water absorption may also be reduced by the shaping method. Application of high pressure during shaping improves densification from the green stage till the sintering stage. Recommendation values of water absorption for building, facing and hollow bricks are given by BIA (2017). The maximum values recommended are 20%, 25% and no limit respectively for bricks exposed to severe, moderate and no weathering.

## CONCLUSION

This study focuses on raw clayey material for fired bricks located in Bomkoul-PK17, Douala in Cameroon, where two main clayey facies have been observed: mottled reddish brown/yellow grey clayey material from surface "A" and the deep blackish grey clayey material "B". Reserve estimation is ~ 1.400.000 tons of clayey material and could supply a small bricks production unit for more than 25 years.

The two facies are dominated by quartz (47-49%) and kaolinite (35-49%) associated with illite (11-1%). Minor K-Feldspar (~3.5%) and traces of hematite (<1%) are also present in facies A. The B facies is richer in sand than the A facies. Chemical analysis is in accord with the mineralogical composition, showing SiO<sub>2</sub> (71–76%), Al<sub>2</sub>O<sub>3</sub> (14%), and Fe<sub>2</sub>O<sub>3</sub> (1–3%).

The fired products obtained from facies "B" showed a matte sound and presented flexural strength < 1.5 MPa, linear shrinkage < 1% and an irregular water absorption i.e evolving in sawtooth pattern with temperature.

Firing products obtained from facies "A" and mixtures obtained from "A" and "B" showed metallic sound, linear shrinkage (1 and 6%) and flexural strength (1.5 and 7 MPa). Water absorption characteristics of the mixtures are suitable for the manufacture of bricks after firing at 1050°C. At this temperature, the firing products present moderate flexural strength (2-3.6 MPa). The M1 mixture (40% of facies A + 60% of facies B) can be used as a satisfactory mixture for a rational use of the different facies of the Bomkoul clayey deposit.

**Acknowledgments:** The authors thank Local Materials Promotion Authority for his financial input during field trips and some characterizations. Grateful acknowledgements are given to Ing. Joël Otten of Laboratory AGEs (University of Liège, Belgium) for X-ray diffraction and thermal analyses.

## References

- Abdulrahman, H. (2015). The dynamic cone penetration test: a review and applications. International Conference on Advances in Civil and Environmental Engineering 2015. DOI: 10.13140/RG.2.2.13275.46882
- Alabduljabbar, H., Benjeddou, O., Soussi, C., Khadimallah, M.A., Alyousef, R. (2021). Effects of incorporating wood sawdust on the firing program and the physical and mechanical properties of fired clay bricks. Journal of Building Engineering, 35,102106. <https://doi.org/10.1016/j.jobbe.2020.102106>

- Andji, J., Abba Toure, A., Kra, G., Jumas, J., Yvon, J., Blanchart, P. (2009). Iron role on mechanical properties of ceramics with clays from Ivory Coast. *Ceram. Int.* 35 571-577.
- Arianpour, A.C., Arianpour, F. (2022). Characterization, technological properties, and ceramic applications of Kastamonu alluvial clays (Northern Turkey) in building materials. *Construction and Building Materials*, 356, 129304. <https://doi.org/10.1016/j.conbuildmat.2022.129304>
- Bain, J.A. & Highley D.E. (1978) Regional appraisal of clay resources: a challenge to the clay mineralogist. In: *International Clay Conference, 1978*, (MM. Mortland & V.C. Farmer eds). *Developments in Sedimentology*, 27, Elsevier, Amsterdam, pp. 437-446.
- Baran B., Ertürk T., Sarikaya Y., Alemdaroglu T. (2001). Workability test method for metals applied to examine a workability measure (plastic limit) for clays. *Appl. Clay Sci.*, 20, 53-63.
- BIA-Bricks Industry Association (2017). Specifications for and classification of brick. Technical Notes, 9A, Reston, Virginia, pp 1-13.
- Boussen S., Sghaier D., Chaabani F., Jamoussi J., Bennour A. (2016). Characteristics and industrial application of the Lower Cretaceous clay deposits (Bouhedma Formation), Southeast Tunisia: potential use for the manufacturing of ceramic tiles and bricks. *Appl. Clay Sci.*, 123 (2016), pp. 210-221. <https://doi.org/10.1016/j.clay.2016.01.027>
- Carretero, M.I., Dondi, M., Fabbri, B., Raimondo, M. (2002). The influence of shaping and firing technology on ceramic properties of calcareous and non-calcareous illitic-chloritic clays. *Appl. Clay Sci.* 20, 301–306. [https://doi.org/10.1016/S0169-1317\(01\)00076-X](https://doi.org/10.1016/S0169-1317(01)00076-X)
- Christidis G.E. (2011) *Advances in the Characterization of Industrial Clays*. EMU Notes in Mineralogy, 9, European Mineralogical Union, Mineralogical Society of Great Britain and Ireland. 341 pp. <https://doi.org/10.1180/EMU-notes.9.9>
- Dondi, M., Fabbri, B., Guarini, G. (1998). Grain-size distribution of Italian raw materials for building clay products: are appraisal of the Winkler diagram. *Clay Miner.* 33,435–442. <https://doi.org/10.1180/000985598545732>
- Dondi, M., Guarini, G., Ligas, P., Palomba, M., Raimondo, M. (2001). Chemical, mineralogical and ceramic properties of kaolinitic materials from the Tresnuraghes mining district. Western Sardinia, Italy. *Appl. Clay Sci.*18,145–155. [https://doi.org/10.1016/S0169-1317\(00\)00042-9](https://doi.org/10.1016/S0169-1317(00)00042-9)

- El Boudour El Idrissi H., Daoudi L., El Ouahabi M., Collin F., Fagel N. (2018). The influence of clay composition and lithology on the industrial potential of earthenware. *Construction and Building Materials*, 172, 650–659. <https://doi.org/10.1016/j.conbuildmat.2018.04.019>
- El Idrissi H., Wafaa B., L. Daoudi, N. Fagel, R. Hakkou, Y. Taha, Y. Tamraoui (2022). An Easy Way for Ceramic Bricks Elaboration to Carry out Basic Technical Measurements. *Advanced Materials Research*, Vol. 1174, pp 3-14. <https://doi.org/10.4028/p-e218c0>
- Elimbi, A., Njopwouo, D. (2002). Firing characteristics of ceramics from the Bomkoul kaolinite clay deposit (Cameroon). *Tile and Brick International*, 18 (6), 364–369. <https://doi.org/10.3390/min14090869>
- Elimbi A., Dika J.M., Djangang C.N. (2014). Effects of Alkaline Additives on the Thermal Behavior and Properties of Cameroonian Poorly Fluxing Clay Ceramics. *Journal of Minerals and Materials Characterization and Engineering*, 2, 484-501. DOI: 10.4236/jmmce.2014.25049
- El Ouahabi M., El Boudour El Idrissi H, Daoudi L., El Halima M., Fagel N. (2019). Moroccan clay deposits: Physico-chemical properties in view of provenance studies on ancient ceramics. <https://doi.org/10.1016/j.clay.2019.02.019>
- Fagel N. (2024a). Climatic significance of clay minerals in Cenozoic marine and lacustrine sediments. *Clay Minerals*, 1–30. doi:10.1180/clm.2024.17
- Fagel N., Israde-Alcantara I., Safaierad R., Rantala M., Schmidt S., Lepoint G., Pellenard P., Mattielli N., Metcalfe S. (2024b). Environmental significance of kaolinite variability over the last centuries in crater lake sediments from Central Mexico. *Applied Clay Science*, 247, 107211. <https://doi.org/10.1016/j.clay.2023.107211>
- Glover P.W.J., Baud P., Darot M., Meredith P.G., Boon S.A., LeRavalec M., Zoussi S., Reuschlé T. (1995).  $\alpha/\beta$  phase transition in quartz monitored using acoustic emissions. *Geophysical Journal International*, Vol. 120 (3) 775–782. <https://doi.org/10.1111/j.1365-246X.1995.tb01852.x>
- Kakali G, Perraki T, Tsivilis S, Badogiannis E. (2001). Thermal treatment of kaolin: the effect of mineralogy on the pozzolanic activity. *Applied Clay Science* 20, 73-80. [https://doi.org/10.1016/S0169-1317\(01\)00040-0](https://doi.org/10.1016/S0169-1317(01)00040-0)

- Kankao, O.O., Ngon Ngon, G.F., Tehna, N., Bayiga, E.C., Mbog, M.B., Mbaï, J.S., Etame, J. (2022). Physicochemical and Mineralogical Characterization of Clay Materials in the Douala Coastal Sedimentary Sub-basin (Cameroon, Central Africa). *Journal of Geosciences and Geomatics*, 10, (3), 126-138. <https://doi.org/10.1016/j.conbuildmat.2020.118097>
- Konta, J. and Künher, R.A., (1997). Integrated exploration of clay deposits: some changes of strategy. *Appl. Clay Sci.* 11,273–283. [https://doi.org/10.1016/S0169-1317\(96\)00027-0](https://doi.org/10.1016/S0169-1317(96)00027-0)
- Lemougna N. Patrick, Arnold Ismailov, Erkki Levanen, Pekka Tanskanen, Juho Yliniemi, Katja Kilpimaa, Mirja Illikainen, (2024). Upcycling glass wool and spodumene tailings in building ceramics from kaolinitic and illitic clay. *Journal of Building Engineering*, vol 81,108122. <https://doi.org/10.1016/j.jobbe.2023.108122>
- Jeridi, K., Hachani, M., Hajjaji, W., Moussi, B., Medhioub, M., Lopez-Galindo, A., Kooli, F., Zargouni, F., Labrincha, J., Jamoussi, F. (2008). Technological behaviour of some Tunisian clays prepared by dry ceramic processing. *Clay Minerals*, 43, 339–350. <https://doi.org/10.1180/claymin.2008.043.3.01>
- Manning, D.A.C. (1995). *Introduction to industrial minerals*. Chapman & Hall Ed., London, 275. ISBN-10: 0-412-55550-6.
- Miall, A.D. (1996). *The Geology of Fluvial Deposits: Sedimentary Facies Basin Analysis, and Petroleum Geology*. Springer-Verlag, 582 p.
- Moore, D.M., Reynolds, R.C., 1989. *X-Ray Diffraction and the identification and analysis of clay minerals*. Oxford University Press, Oxford, 332 pp.
- NC 23-2010 : Spécifications techniques pour briques de terre cuite, 8p.
- Ngon Ngon G.F., Yongue Fouateu R., Lecomte Nana G.L., Bitom L.D., Bilong P., Lecomte G. (2012a). Study of physical and mechanical applications on ceramics of the lateritic and alluvial clayey mixtures of the Yaoundé region (Cameroon). *Construction and Building Materials*, 31, 294–299. doi:10.1016/j.conbuildmat.2011.12.108
- Ngon Ngon, G.F., Etame, J. Ntamak-Nida, M.J. Mbog, M.B. Mpondo, A.M M. Gerard, M. Yongue Fouateu R., Bilong P. (2012b). Geological study of sedimentary clayey materials of the Bomkoul area in the Douala region (Douala sub-basin, Cameroon) for the ceramic industry. *C.R. Geoscience*, 344, 366–376. <https://doi.org/10.1016/j.crte.2012.05.004>

- Nguene, F.R., Tamfu, S., Loule, J.P., Ngassa, C. (1992). Paléoenvironnement of the Douala and Kribi/Campo subasins in Cameroon West Africa. In Curnelle, R. ed., *Géologie Africaine*, 1er Coll. de stratigraphie et paléogéographie des bassins sédimentaires ouest africains, 2<sup>ème</sup> coll. africain de micropaléont, Libreville, 1001, BousSENS, Elf Aquitaine, 129-139.
- Nzeukou Nzeugang A, Medjo Eko R, Fagel N, Kamgang Kabeyene V, Njoya A, Balo Madi A, Mache J-R, Melo Chinje U. Characterization of clay deposits of Nanga-Eboko (Central Cameroon): Suitability in the production of building materials. *Clay Min.* 2013;48: 655–662. <https://doi.org/10.1180/claymin.2013.048.4.18>
- Pialy P., Nkoumbou C., Villiéras F., Razaftianamaharavo A., Barres O., Pelletier M., Ollivier G., Bihannic I., Njopwouo D., Yvon J., Bonnet J.P. (2008) Characterization for the industrial applications of clays from Lembo deposit, Mount Bana (Cameroon). *Clay Minerals*, 43:415–436. <https://doi.org/10.1180/claymin.2008.043.3.07>
- Regnault, J.M. (1986). *Synthèse Géologique du Cameroun DMG*. Yaoundé, 199 p.
- Reeves, G.M., Sims, I., Cripps, J.C. (2006). *Clay Materials Used in Construction*. Geological Society, London (525pp.).
- Saikia B.J., Parthasarathy G. (2010). Fourier Transform Infrared Spectroscopic Characterization of Kaolinite from Assam and Meghalaya, Northeastern India, *J. Mod. Phys.* 1, 206-210. DOI: 10.4236/jmp.2010.14031.
- SNH/UD, (2005). *Stratigraphie séquentielle et tectonique des dépôts mésozoïques synrifts du Bassin de Kribi/Campo*. M.J. Ntamak-Nida, B. Ketchemen-Tandia, J.E. Mpesse, S. Ndong Ondo, P. Courville, F. Baudin, Rapport inédit, 2005, 134p, 11 planches, 02 Rap. Annexes d'analyses.
- Sobdjou, C.K., Mfayakouo, BC, Ngueutchoua, G., Kenfack, RGN, Ngoss, III S. (2023). Paléoenvironnement of the Albian-Cenomanian Mundeck Formation in the Douala Basin (SW, Cameroon): Evidence from facies analysis and geochemistry. *Geological Journal*, 1-21. <https://doi.org/10.1002/gj.4710>
- Tchakoute H.K., Mbey J.A., Elimbi A., Kenne D.B.B., Njopwouo D. (2013). Synthesis of volcanic ash-based geopolymer mortars by fusion method: Effects of adding metakaolin to fused volcanic ash. *Ceramics International* 39, 1613-1621. <https://doi.org/10.1016/j.ceramint.2012.08.003>
- Thibault, P.M., Le Berre, P. (1985). *Les argiles pour brique*. BRGM.CRMO-85. MIMEE, Yaoundé Cameroun, 65p.

- Tsozué, Désiré, Nzeukou Nzeugang, Aubin; Mache, Jacques Richard, Fagel Nathalie (2017). Mineralogical, physico-chemical and technological characterization of clays from Maroua (Far-North, Cameroon) for use in ceramic bricks production. *Journal of Building Engineering*, 11, p. 17-24. <https://doi.org/10.1016/j.jobbe.2017.03.008>
- Walker R.G. (2006). Facies models revisited. *in* Henry W. Posamentier & Roger G. Walker Editor(s), Doi:<https://doi.org/10.2110/pec.06.84.0001>; SEPM Society for Sedimentary Geology, Vol. 84, ISBN print: 9781565763302.
- Wang S., Gainey L., Mackinnon I.D.R., Allen C., Gu Y., Xi Y. (2023). Thermal behaviors of clay minerals as key components and additives for fired brick properties: A review. *Journal of Building Engineering*, 66,105802. <https://doi.org/10.1016/j.jobbe.2022.105802>

Figure 1: (a) Geological sketch map of Douala sub-basin, SNH/UD-2005 (after [Ngon Ngon et al. \(2012b\)](#)); (b) Potential areas of clayey deposits in Douala sub-basin, BRGM-1985; (c) General view of Bomkoul's clayey deposits-Google map

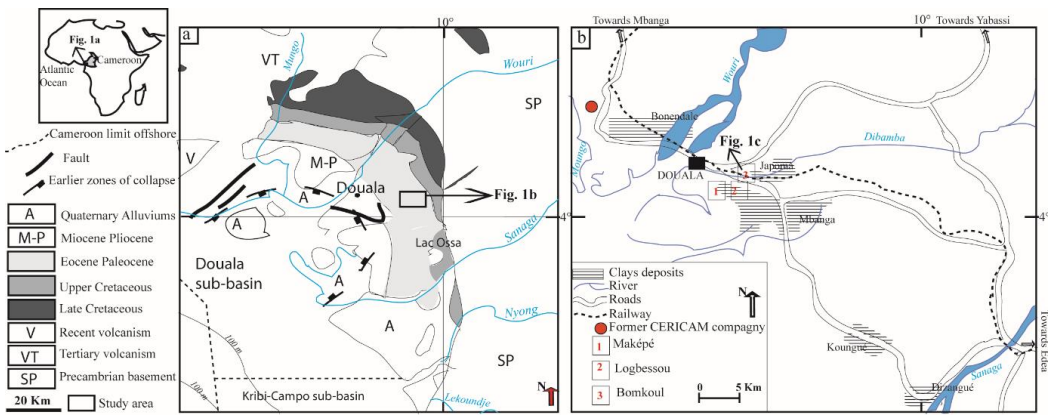


Figure 2: Sampling points and drilling position (SPT1-SPT2) on the new clayey site at Bomkoul

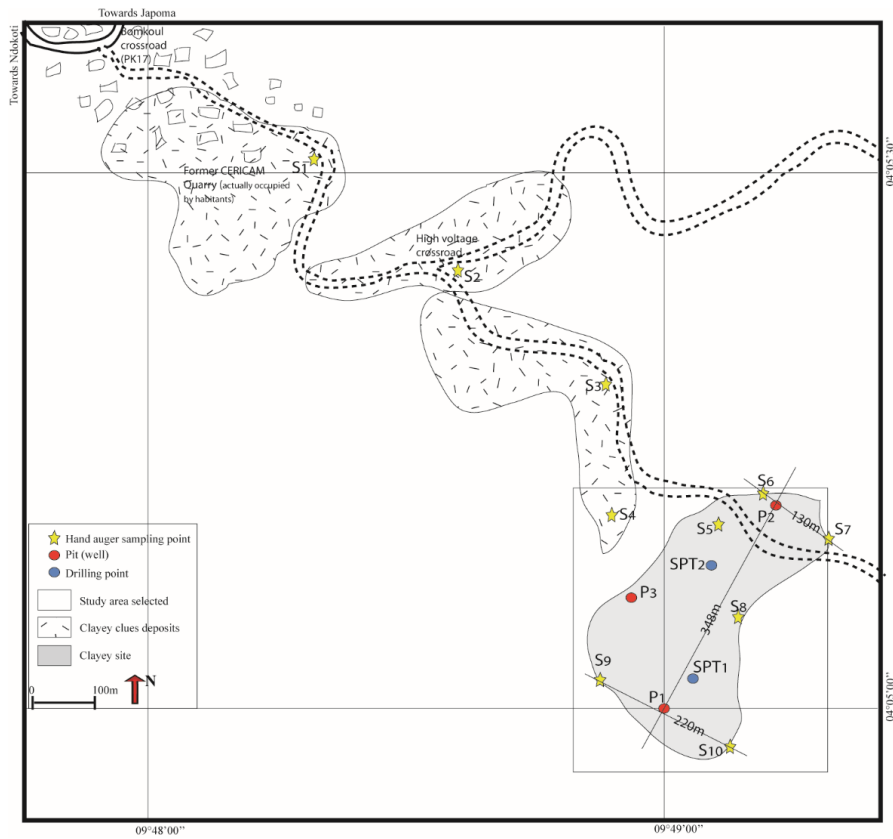


Figure 3: (a) Stratigraphic column of Douala Basin (from Sobdjou et al., 2023), (b) Drilling log of Bomkoul's clayey materials (PEI: non perturbed sample; A and B are two major layers observed in the site and used for technological tests)

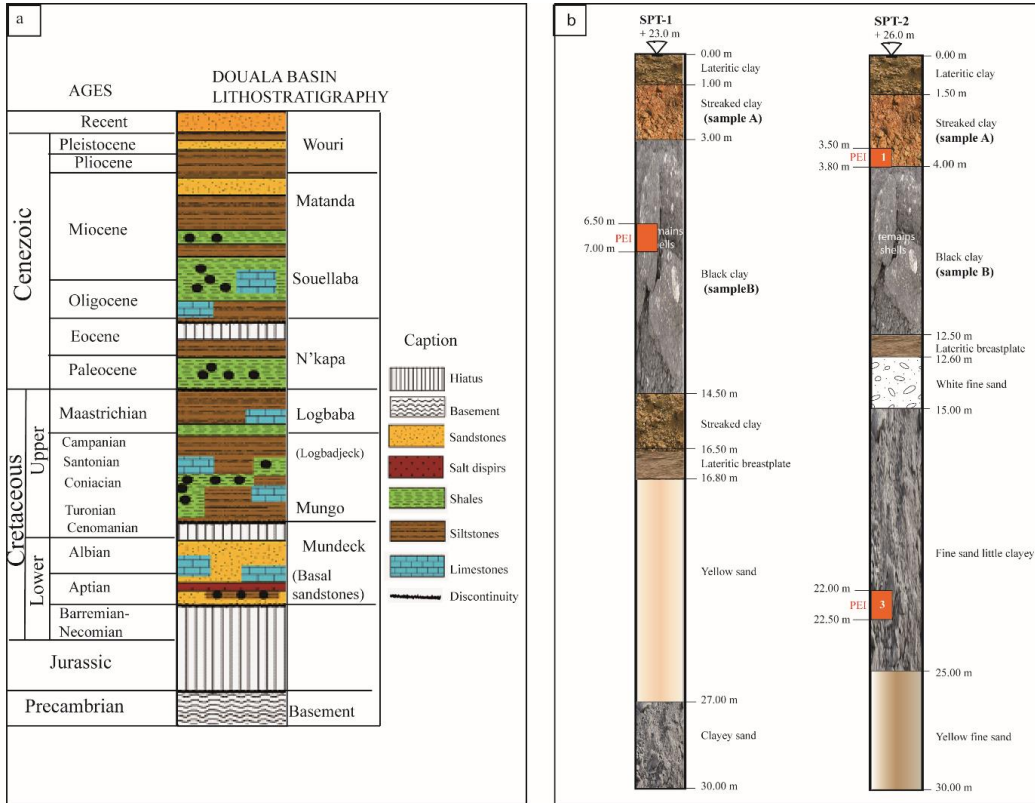


Figure 4: (a) XRD trace of bulk samples, (b) and (c) Clay XRD trace of clay fractions of Bomkoul's clayey materials; N: Air dried samples; EG: ethylene glycol solvated samples; 500°C: heated samples

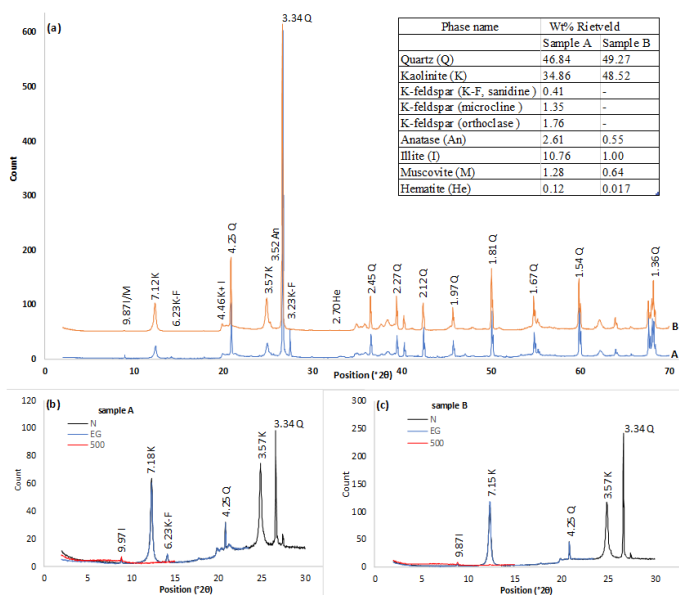


Figure 5: FTIR spectra of some studied clayey materials

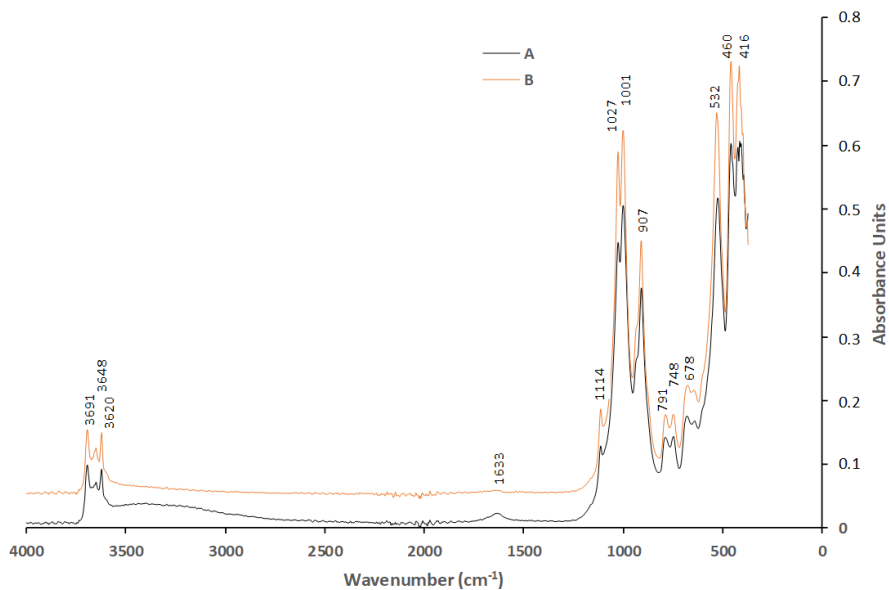


Figure 6. STA analysis of the studied samples

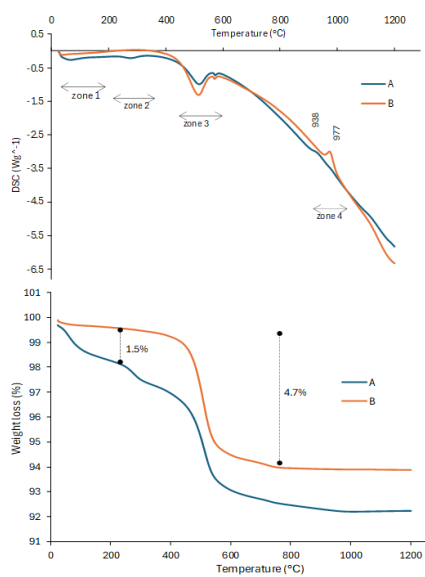


Figure 7: (a) Particle size curves of the Bomkoul's clay; projection of samples in: (b) Holtz and Kovacs diagram, (c) Bain and Highley (1978) diagram

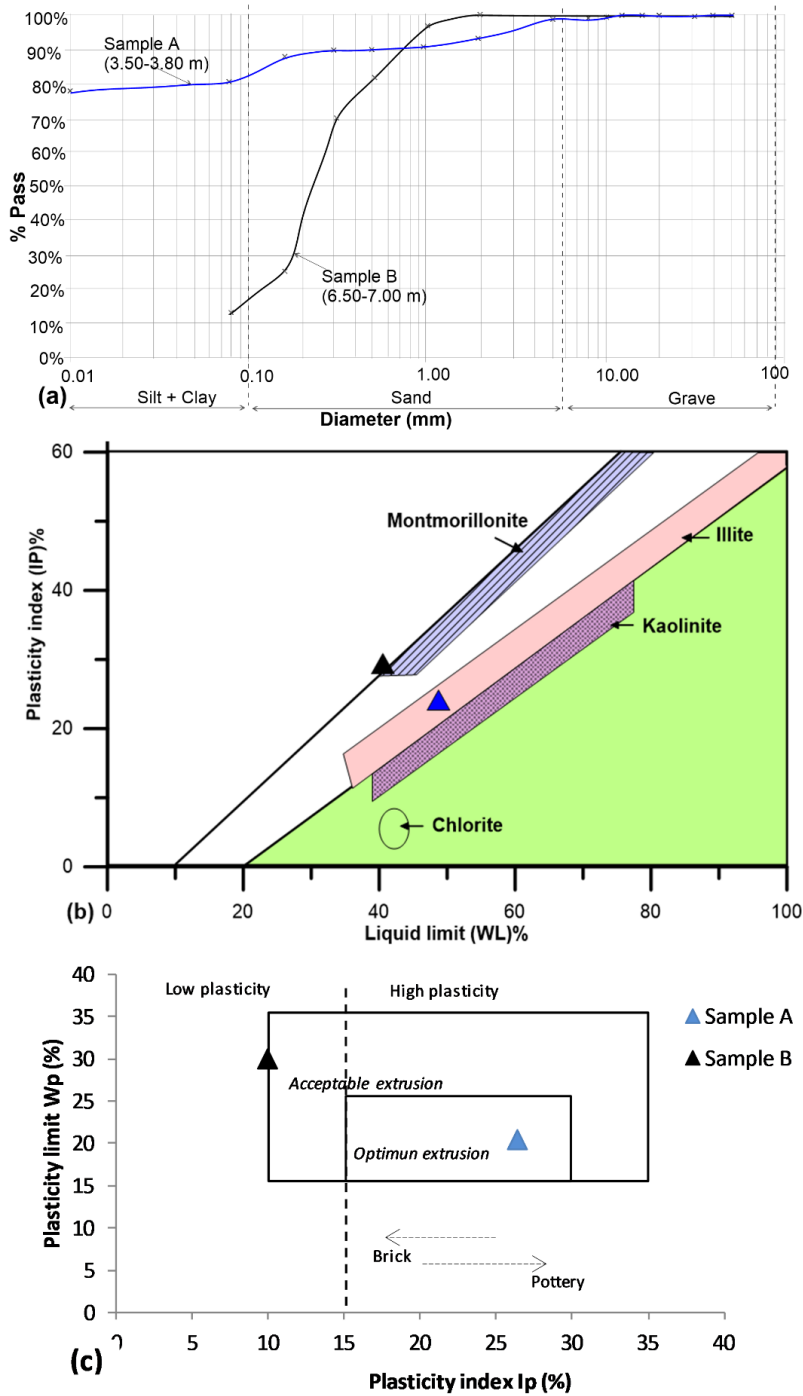


Figure 8: Shear stresses vs volume deformation

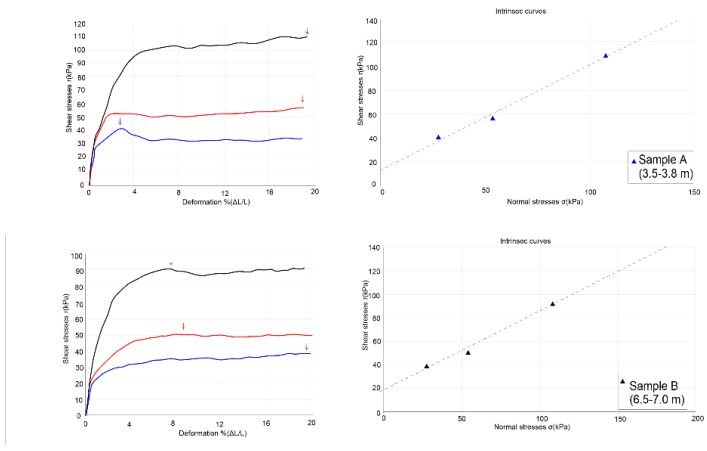
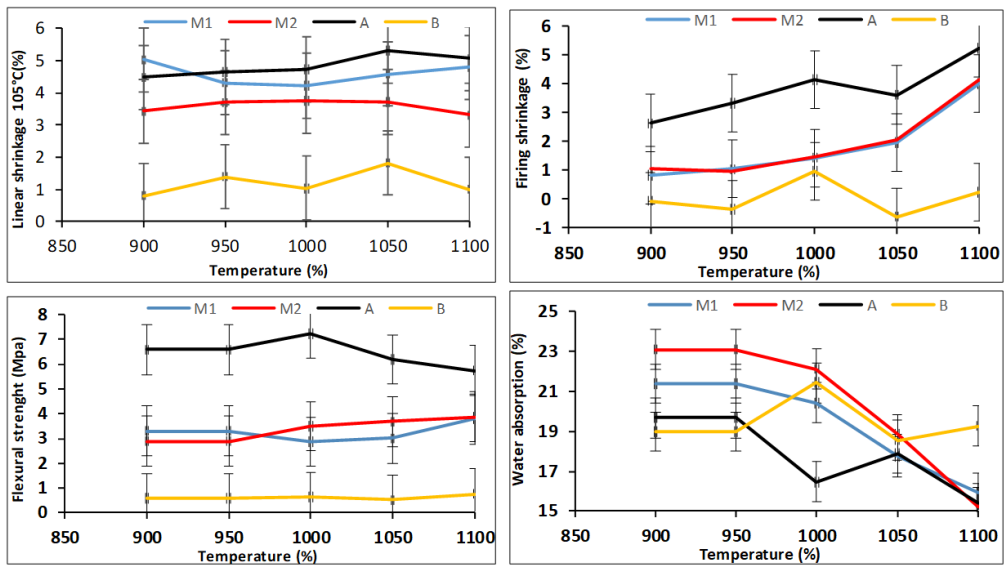


Figure 9: Evolution of firing properties of the clayey specimens with temperature



### Table captions

Table 1: Reserve evaluation of Bomkoul' clayey materials

Table 2: Major chemical composition (wt%) of Bomkoul clayey materials. LOI: Loss on ignition at 1000°C for 2h

Table 3: Geotechnical properties of Bomkoul' clayey materials

Table 4: Technological properties of fired bricks from Bomkoul's clayey materials

### Supplementary Materials:

Fig. 1S: Photos of the majors two facies observed at Bomkoul's clayey deposit

Fig. 2S: Rietveld refinement image obtained

Fig. 3S: Resistance of the terrain with deep

Fig. 4S: Specimens of fired bricks

Table 1: Reserve estimation of Bomkoul' clayey materials

	Thickness (m)	Average density* (t/m <sup>3</sup> )	Average area (m <sup>2</sup> )	Volume (m <sup>3</sup> )	Deposit (t)	Exploitation (t/yr)	Extracted clay time (Year)
Facies "A"	2	1.6	60 000	120 000	192 000	50000	3.8
	2.5			150 000	240 000		4.8
Facies "B"	8.5			510 000	816 000		16.3
	11.5			690 000	1 104 000		22.1

\*The density of clayey material was considered to be 1.6 t/m<sup>3</sup>; facies A and facies B have densities 1.6 and 1.7 t/m<sup>3</sup> respectively

Table 2: Major chemical composition (wt%) of Bomkoul clayey materials. LOI: Loss on ignition at 1000°C for 2h

Colour	Facies	SiO <sub>2</sub>	Al <sub>2</sub> O <sub>3</sub>	Fe <sub>2</sub> O <sub>3</sub>	MgO	CaO	Na <sub>2</sub> O	K <sub>2</sub> O	TiO <sub>2</sub>	P <sub>2</sub> O <sub>5</sub>	LOI	Total
Mottled red/yellow grey	A	76.40	14.27	1.35	0.00	0.17	0.17	0.13	1.49	0.03	5.53	99.54
Grey / Dark grey	B	71.15	13.62	2.86	0.36	0.22	0.18	0.85	1.47	0.06	8.55	99.32

Table 3: Geotechnical properties of Bomkoul' clayey materials

Characteristics	Sample A (SPT-2)	Sample B (SPT-1)
Depth (m)	3.50 – 3.80	6.50 – 7.00
Nature of sample	Undisturbed	Undisturbed
Water content (%)	41.4	19.4
<i>Volumetric weight (kN/m<sup>3</sup>)</i>		
Unit weight- $\gamma_h$	15.9	18.9
Dry unit weight- $\gamma_d$	11.2	15.9
Specific unit weight- $\gamma_s$ (T/m <sup>3</sup> )	2.62	2.65
<i>Particle size</i>		
% passing <20mm	100.0	100.0
<10 mm	99.3	100.0
<5 mm	98.6	100.0
<2 mm	93.4	100.0
<1 mm	91.0	97.2
<0.315 mm	89.3	70.7
<80 $\mu$ m	80.6	13.5
Grave (%)	1.40	0.00
Sand (%)	18.0	86.5
Fine (%)	80.6	13.5
<i>Plasticity (%)</i>		
Liquidity limit-LL	46.9	40
Plasticity index-IP	20.4	30
Liquidity index-I <sub>L</sub>	0.732	0.313
<i>Direct shear strength-UU</i>		
Cohesion: Cu (kPa)	13.1	17.4
Friction angle: $\phi_u$ (°)	41.3	34.1
<i>AASHTO classification</i>	A-7-6(13)	A-2-4(0)
	Plastic material	Sandy material

Table 4: Technological properties of fired bricks from Bomkoul's clayey materials

Firing temperature	Mixture samples	Linear shrinkage (L <sub>105°C</sub> , %)	Colour & Cohesion	Sonority	Firing shrinkage (%)	Flexural strength (N/mm <sup>2</sup> )	Water absorption (%)
900	M1	5.0	Pink & good	Metallic	0.8	3.3	21.3
	M2	3.4		Metallic	1.1	2.9	23.1
	100% <sub>A</sub>	4.4		Metallic	2.6	6.6	19.7
	100% <sub>B</sub>	0.8		Dull	-0,061	0.6	18.9
950	M1	4.3	Pink & good	Metallic	1.0	3.3	21.4
	M2	3.7		Metallic	0.9	2.9	23.1
	100% <sub>A</sub>	4.6		Metallic	3.3	6.6	19.7
	100% <sub>B</sub>	1.4		Dull	-0.3	0.6	18.9
1000	M1	4.2	Pink & good	Metallic	1.4	2.1	20.4
	M2	3.7		Metallic	1.5	3.5	22.1
	100% <sub>A</sub>	4.7		Metallic	4.1	7.2	16.5
	100% <sub>B</sub>	1.0		Dull	0.9	0.6	21.4
1050	M1	4.6	Pink & good	Metallic	1.9	3.0	17.7
	M2	3.7		Metallic	2.1	3.7	18.8
	100% <sub>A</sub>	5.3		Metallic	3.6	6.2	17.1
	100% <sub>B</sub>	1.8		Dull	-0.6	0.5	18.6
1100	M1	4.7	Pink & good	Metallic	4.0	3.8	15.9
	M2	3.3		Metallic	4.1	3.9	15.2
	100% <sub>A</sub>	5.4		Metallic	5.2	5.75	15.4
	100% <sub>B</sub>	1.0		Dull	0.2	0.77	19.3